Eur. Phys. J. B **10**, 705–718 (1999)

THE EUROPEAN PHYSICAL JOURNAL B

EDP Sciences

Diffusion and rheology in a model of glassy materials

R.M.L. Evans[a], M.E. Cates, and P. Sollich[b]

Department of Physics & Astronomy, The University of Edinburgh, JCMB King's Buildings, Mayfield Road, Edinburgh EH9 3JZ, UK

Received 31 August 1998 and Received in final form 25 January 1999

Abstract. We study self-diffusion within a simple hopping model for glassy materials. (The model is Bouchaud's model of glasses (J.-P. Bouchaud, J. Phys. I France **2**, 1705 (1992)), as extended to describe rheological properties (P. Sollich, F. Lequeux, P. Hébraud, M.E. Cates, Phys. Rev. Lett. **78**, 2020 (1997)).) We investigate the breakdown, near the glass transition, of the (generalized) Stokes-Einstein relation between self-diffusion of a tracer particle and the (frequency-dependent) viscosity of the system as a whole. This stems from the presence of a broad distribution of relaxation times of which different moments control diffusion and rheology. We also investigate the effect of flow (oscillatory shear) on self-diffusion and show that this causes a finite diffusivity in the temperature regime below the glass transition (where this was previously zero). At higher temperatures the diffusivity is enhanced by a power law frequency dependence that also characterises the rheological response. The relevance of these findings to soft glassy materials (foams, emulsions etc.) as well as to conventional glass-forming liquids is discussed.

PACS. 64.70.Pf Glass transitions – 66.10.Cb Diffusion and thermal diffusion – 83.50.Fc Linear viscoelasticity

1 Introduction

The dynamics of systems close to a glass transition remains a central problem in statistical physics [1]. Because the glass transition is a many-body phenomenon, models for it invariably involve some approximation and it is important to disentangle the physical phenomena from the approximation scheme used. In mode-coupling theories, for example, the dynamics are dominated by a small number of collective degrees of freedom [2]. This is appealing, but ignores activated processes, and obscures the fact that glassy materials are dynamically heterogeneous with a variety of local environments [3]. Another approach is to use disordered hopping models, which treat instead single-particle degrees of freedom coupled to a random environment, and this is the route followed here. Such models, though unrealistic in some respects, are likely to give a better account of those properties, such as self-diffusion, which are not dominated by relaxation of collective modes.

An important breakthrough in the approach based on hopping models was that of Bouchaud [4], who showed that an ensemble of *non-interacting* particles, moving by thermally activated hopping at temperature T in an uncorrelated fashion through a sequence of traps, can show a glass transition. This occurs if and only if the density of states (the prior probability distribution of trap depths) $\rho(E)$ has an exponential tail. Though grossly oversimplified, this allows many properties of the model to be calculated exactly. The exponential tail to the prior distribution $\rho(E)$, which leads to a power-law spectrum of relaxation times and is vital to the appearance of a glass transition, is supported by evidence from theory on spin glasses [5] and experiments on low-temperature fluids [6]. Such a power-law relaxation spectrum was the point of departure for a related model of glasses [7,8], and similar features appear in models of dispersive transport in disordered semiconductors [9].

The original model of Bouchaud has no explicit spatial coordinates. Nevertheless, the extension to self-diffusion is unambiguous (if each hop corresponds to a spatial displacement with a well-defined second moment) and indeed Monthus and Bouchaud [10] gave an expression for the distribution of displacements on a hypercubic lattice. For flow properties, more choices are possible in the way spatial coordinates are treated, but a minimal extension of the model was offered by Sollich *et al.* [11,12]. This model, which we call the GR (glassy rheology) model allows both linear and nonlinear rheological properties to be calculated. Details of it are recalled in Section 3 below.

The model introduced in reference [11] was in fact proposed to describe a class of "soft glassy materials" (argued to include foams, dense emulsions, etc.), in which context it was found necessary to replace the thermodynamic temperature T in Bouchaud's model by an effective (noise) temperature $x \gg T$. This replacement converts the GR

[a] e-mail: R.M.L.Evans@ed.ac.uk

[b] *Present address*: Department of Mathematics, King's College, University of London, London, WC2R 2LS, UK

model studied below into the *soft* glassy rheology model of references [11,12], and can be made throughout our calculations.

The glass transition in the GR model shows interesting features which may need further explanation for readers whose background lies in conventional glasses. Specifically, in Bouchaud's model the glass transition T_g is identified as the temperature below which the system shows "weak ergodicity breaking": its Boltzmann distribution is not normalizable. This means the system will evolve into deeper and deeper traps as time goes by, and will never attain a steady state — although at no finite time are there infinite barriers partitioning phase space. When flow-related degrees of freedom are included in the model (see Sect. 3 below), one finds, as expected, that the system has a finite elastic modulus (at zero frequency) for temperatures $T < T_g$. Less obviously, the *viscosity* of the material diverges, not at $T = T_g$ but at $T = 2T_g$. Between these two temperatures, the static modulus is zero but the viscosity infinite; the material is what is known in rheological language as a "power-law fluid". For applications of the model to soft glassy materials this is a very attractive feature, since such viscoelastic behaviour is frequently observed in these systems [11,12]. In a model of conventional glasses, on the other hand, it might be considered undesirable. However, with the introduction of a high energy cutoff in the prior distribution $\rho(E)$, the phenomenology of the GR model can be adapted to model that of conventional glasses. We discuss the conceptual features of this modification at the end of Section 7; for the actual calculations in the present paper we restrict ourselves to the simpler case without cutoff.

Below we calculate the statistics (additional to the results of Ref. [10]) of self-diffusion in the GR model, and explore quantitatively the breakdown, near the glass transition, of the (generalized) Stokes-Einstein relation [(G)SER] between self-diffusion of a representative particle in the fluid and the (frequency-dependent) viscosity of the system as a whole. (This breakdown does not, of course, imply that GSER also fails for *macroscopic* probe particles which see the surrounding material as a continuum.) We also investigate the effect of shear flow on self-diffusion and show that this causes a finite diffusivity in the low-temperature regime where this was previously zero.

In the next section we review the status of the GSER in both conventional and soft glassy systems. The GR model is described in Section 3 and used in Section 4 to study and discuss the breakdown of the GSER. In Section 5, we further elucidate the physics of particle transport in glassy systems, using both analysis and simulation of the model. In Section 6 we calculate the effects of shear on the rate of self-diffusion, finding the diffusion constant in the presence of continuous and periodic shear strains of various rates and amplitudes. In Section 7 we conclude with a discussion of our results in the context of both conventional super-cooled/glass-forming liquids and soft glassy materials.

2 Stokes-Einstein relation

The Stokes-Einstein relation (SER) between coefficients of diffusion and viscosity (and its generalization to frequency-dependent quantities) is of great importance to our understanding of transport in fluids. This is especially true since the development of new techniques to measure viscoelastic response by light scattering from (or tracking of) probe particles [13–15]. Yet the relation's range of validity has been called into question by experiments on super-cooled and glass-forming liquids [16–21].

To find the linear storage and loss moduli, $G'(\omega)$ and $G''(\omega)$, of a viscoelastic fluid, a rheometer is normally used to apply an oscillatory stress to the fluid and measure the resultant strain (or *vice versa*) as a function of (angular) frequency ω. A technique has recently been developed whereby the complex viscoelastic modulus G^* ($\equiv G' + \mathrm{i}G''$) may be found[1], even when the available sample of fluid is too small to fill a rheometer. The technique involves introducing one or more neutrally buoyant probe spheres of radius a into the fluid and measuring their Brownian motion. For a Newtonian fluid, which is characterized by a single, frequency-independent viscosity η, that viscosity is given by the familiar Stokes-Einstein formula $\eta = k_B T/6\pi a D$. Here k_B is Boltzmann's constant and T temperature. As the fluid is Newtonian, the probe executes an unbiased random walk, and its mean-square displacement as a function of time is $\langle r^2(t)\rangle = 6Dt$, which defines the diffusion constant D appearing in the Stokes-Einstein formula. In this purely viscous fluid, G^* is purely imaginary, given by $G^*(\omega) = \mathrm{i}\omega\eta$. As the derivative of the stress relaxation modulus is a well-behaved function of time, its Laplace transform $\widetilde{G}(s)$ is simply related to its Fourier transform $G^*(\omega) = \widetilde{G}(\mathrm{i}\omega)$. Combining the above expressions, we see that probe spheres *in a Newtonian fluid* respect the relation

$$\widetilde{G}(s) = \frac{k_B T}{\pi a s \langle \widetilde{r^2}(s)\rangle} \tag{1}$$

where $\langle \widetilde{r^2}(s)\rangle$ is the Laplace transform of the mean-square displacement of a probe. Equation (1) says that the modulus of a viscoelastic fluid is the ratio of a driving force (in this case induced by $k_B T$ rather than by a rheometer) to a response (mean-square distance moved by the sphere).

Although derived above only for the Newtonian case, equation (1) is the generalized Stokes-Einstein relation (GSER), and when written in this form it applies under relatively general conditions[2] to *all linearly viscoelastic fluids*, not just Newtonian ones [14]. The basic Stokes-Einstein relation (SER) is recovered from equation (1) in the zero frequency limit, since viscosity is *defined* by $\eta \equiv \lim_{\omega\to 0} G''(\omega)/\omega$. In all cases, the fluid around

[1] $G^*(\omega)$ is the Fourier transform of the time derivative of the stress relaxation modulus $G_r(t)$, which relates stress on the fluid, $\sigma(t) = \int_0^t \mathrm{d}t_1 G_r(t-t_1)\dot{\gamma}(t_1)$, to strain rate $\dot{\gamma}(t)$.

[2] At sufficiently high frequency, for a probe of finite mass, the modulus has an additional inertial contribution which we drop.

the probe is treated as a featureless continuum, and therefore the result is only valid when the sphere radius greatly exceeds the microscopic length scale (*e.g.* particle size) of the fluid. (Furthermore, probe particles must be sufficiently dilute to ensure independent Stokesian flow fields around each.) If, as is sometimes the case, the GSER is applied to probe particles which are not large compared to the microscopic scale, then it ceases to be a rigorous result. As an approximation, it is then close to the spirit of effective medium theory (wherein a representative particle is viewed as embedded in a continuum and its contribution to the continuum properties then calculated self-consistently).

With macroscopic probe particles, the GSER has been fruitfully employed [13,14] to measure the rheological properties of viscoelastic fluids from light scattering or optical tracking observations of the suspended probes. In reference [15], Mason and Weitz applied this method successfully to various systems, using colloidal spheres as probes. Remarkably, in one case the medium analysed was itself a suspension of the colloidal particles, of volume fraction $\phi = 0.56$, which lies close to the glass transition concentration. The scattering method used was diffusion-wave spectroscopy (DWS) [22] whose direct interpretation in terms of self-diffusion is somewhat ambiguous; but in any case, both criteria for the rigorous validity of the GSER were violated (no separation of length scales, and probe particles not dilute). Yet the diffusion data for this system, analysed as though DWS was probing self-diffusion and transformed into putative rheological data *via* the GSER, compare remarkably well with frequency-dependent rheological data measured directly. Among various explanations that are possible for this, is the idea that the GSER is in fact more widely valid than generally assumed [15].

On the other hand, in conventional glass-forming fluids, the (zero-frequency) tracer diffusion and viscosity have been measured as a function of temperature, by experiment [16–21] and simulation [23]. While the SER held (within a factor of order unity) for probes just a few times larger than the fluid particles [19], for equal-size probes the translational diffusion was enhanced by orders of magnitude with respect to the SER prediction as the glass transition was approached.

In view of the unexpected success of GSER for colloidal glassy fluids, alongside the failure of SER for conventional glasses[3], a more detailed examination of the connection between diffusion and rheology seems worthwhile, and we pursue this in what follows.

3 The model

We use a simple hopping model to emulate properties of a fluid close to its glass transition. The model, which will be referred to as the "glassy rheology" (GR) model, was defined in reference [11], where its response to a macroscopic shear was calculated. In the present study we shall investigate the relation between rheology and particle transport in the GR model.

3.1 Definition

The GR model is based on Bouchaud's model for glassy dynamics [4], with the addition of shear strain degrees of freedom which that model lacks. Particles in the Bouchaud model are thermally activated at temperature $T = \beta^{-1}$ from traps of energetic depth E in a time τ which has an exponential distribution with rate $\Gamma_0 \exp -(\beta E)$, where Γ_0 is some microscopic rate constant. Having escaped, a particle selects its next trap *at random* (*i.e.* there are no spatial correlations) from the *prior distribution* of trap depths $\rho(E)$. We briefly recall the resulting behaviour of Bouchaud's model. For high temperatures T, the occupancy of traps of depth E evolves towards the Boltzmann distribution $P_{\rm occ}^{\rm eq}(E) \sim \rho(E)\exp(E/T)$. As T is lowered, this distribution may cease to be normalizable, leading to a glass transition at $T_{\rm g}^{-1} = -\lim_{E\to\infty}(\partial/\partial E)\ln\rho(E)$. For $T < T_{\rm g}$, no equilibrium state exists, and the system shows "weak ergodicity breaking" and various ageing phenomena. A finite value of $T_{\rm g}$ implies an exponential tail in the density of states, $\rho \sim \exp(-E/T_{\rm g})$.

The GR model ascribes some internal features to the traps. This is done through a minimalist description in which the tensorial aspects of the problem are ignored and the shear rate and strain are treated as though they were scalar quantities [11,12]. The trap's potential is taken to be quadratic in a local strain (or relative displacement) coordinate l, so that the particle's energy is $\frac{1}{2}kl^2$, with k a constant. This applies up to a local yield value l_y, whose energy $E = \frac{1}{2}k{l_y}^2$ is the depth of the trap. Upon reaching this threshold, the system locally rearranges to a new configuration, thus relaxing the local strain l_y. The yield energy of the new potential well is drawn from the prior distribution $\rho(E)$, and its strain l set to zero. In the absence of an externally imposed shear rate $\dot\gamma$, all l values remain zero, and the GR model reduces to the Bouchaud model, with hopping between traps caused by thermal activation alone. With shear imposed, changes in all local strains are assumed to follow the global strain rate, $\dot l = \dot\gamma$. (This assumption is mean-field in character.) With the particles thus dragged up their quadratic energy wells by global shear, the barrier to thermal activation is reduced, and the local yield rate becomes $\Gamma_0\exp[-\beta(E-\frac{1}{2}kl^2)]$. If $P_{\rm occ}(l,E;t)\,{\rm d}l\,{\rm d}E$ is the probability of finding an occupied trap of given l and E, the above dynamics imply [11,12]

$$\frac{\partial}{\partial t}P_{\rm occ} = -\dot\gamma\frac{\partial}{\partial l}P_{\rm occ} - \Gamma_0 {\rm e}^{-\beta(E-\frac{1}{2}kl^2)}P_{\rm occ} + \Gamma(t)\,\rho(E)\delta(l). \tag{2}$$

The first term on the R.H.S. arises from local straining by the macroscopic deformation. The second describes the loss of occupied traps from the distribution by thermally activated yielding. The last term corresponds to creation of new, unstrained configurations, whose trap depth is

[3] For a related discussion of the failure of Einstein relations in biased diffusion processes, see [24].

drawn from the prior $\rho(E)$, at a rate equal to the total yield rate in the system, $\Gamma(t) = \Gamma_0 \left\langle \exp[-\beta(E - \frac{1}{2}kl^2)] \right\rangle_P$.

Note that, as originally conceived in the context of soft glassy materials [11,12] each occupied trap represented a small region of the medium, large enough for a local shear strain l to be defined, but small enough for this to be approximately uniform within the region. However, the model can readily be interpreted as describing the motion of individual particles in a conventional supercooled/glass-forming fluid, by associating the local strain l with, say, the relative displacement of a particle from the centre of a trap formed by its neighbours.

We have not yet defined the stress in the GR model. Due to stochastic yielding events, the local stress, which we take to be kl, is inhomogeneous (it follows the local strain l, rather than the macroscopic strain). Since we have stated that the strain rate $\dot{l}$ is everywhere equal to the global strain rate $\dot{\gamma}$, these local stresses must combine according to a straightforward average so that $\sigma = k\langle l \rangle \equiv k \int l\, P_{\rm occ}(l, E; t)\, \mathrm{d}l\, \mathrm{d}E$. As discussed in Section 4.1, this corresponds to a fully parallel mechanical circuit; this is the only combination consistent with affine shear, and may well be approached in many physical systems.

3.2 Rheology and diffusion

The dynamics described (Eq. (2)) are further motivated in references [11,12], where the GR model's constitutive relation between stress and strain rate is calculated. We now briefly summarize the linear rheology that the model predicts. We use non-dimensional units for time and energy by setting $\Gamma_0 = T_{\rm g} = 1$; we also re-scale our strain variables (l, γ) and stress σ so that $k = 1$. The complex dynamic shear modulus $G^*(\omega) = G' + \mathrm{i}G''$ describes the stress response to small shear strain perturbations around the equilibrium state. As such, it is well-defined (*i.e.* time-independent) only above the glass transition, $T > 1$. Expanding equation (2) to first order in the amplitude γ_0 of an oscillatory strain $\gamma(t) = \gamma_0 \cos \omega t$, we find

$$G^*(\omega) = \left\langle \frac{\mathrm{i}\omega\overline{\tau}(E)}{\mathrm{i}\omega\overline{\tau}(E) + 1} \right\rangle_{\rm occ} \tag{3}$$

where the average is taken with respect to occupied traps, and $\overline{\tau}(E) = \exp(\beta E)$ is the mean (Arrhenius) residence time for a trap of depth E. (We distinguish this from the actual residence time τ in such a trap, which is a random variable.) Equation (3) corresponds to a distribution of Maxwell modes whose spectrum of relaxation times is given by the equilibrium distribution $P^{\rm eq}_{\rm occ}(E) \sim \exp(\beta E)\rho(E)$. Given that $\rho(E)$ has an exponential tail (required for $T_{\rm g}$ to be finite), the distribution of residence times thus exhibits power-law behaviour for large τ: $\Psi_{\rm occ}(\tau) \sim \tau^{-T}$. This leads to power laws[4] for G^* in the low frequency range:

$$\begin{array}{llll} G' \sim \omega^2 \text{ for } 3 < T, & \sim \omega^{T-1} \text{ for } 1 < T < 3 \\ G'' \sim \omega \text{ for } 2 < T, & \sim \omega^{T-1} \text{ for } 1 < T < 2. \end{array} \tag{4}$$

For $T > 3$ the system is Maxwell-like at low frequencies, whereas for $2 < T < 3$ there is an anomalous power law in the elastic modulus. Most interesting is the regime $1 < T < 2$, where G' and G'' have constant ratio; both vary as ω^{T-1}. Moreover, the frequency exponent approaches zero as $T \to 1$, resulting in essentially constant values of G'' and G'. Note, however, that the ratio $G''/G' \sim T - 1$ becomes small as the glass transition is approached.

This increasing dominance of the elastic response G' prefigures the onset of a yield stress for $T < 1$ [11,12]. However, for $T < 1$ the linear viscoelastic moduli show slow time evolution and ageing effects [25] in accordance with the weak ergodicity breaking discussed in Section 1. Accordingly, in the following section, where the GSER for this model is discussed, we consider only $T > T_{\rm g} = 1$. However, that does include the regime $T_{\rm g} \leq T \leq 2T_{\rm g}$ which would lie below the "glass transition temperature" were this to be defined operationally by the divergence of the viscosity. As $T_{\rm g}$ is approached from above, the equilibration time following a quick quench diverges. Hence, even for $T > T_{\rm g}$, non-equilibrium situations are also of interest in glass-forming materials, though we shall consider only equilibrium situations in the following section.

In order to study self-diffusion [10], we must clarify further the spatial interpretation of our GR model. We shall associate each relaxation event with a step on an unbiased random walk. We draw each step from a Gaussian[5] of unit variance in each spatial direction (thus defining a length unit for the model). This gives a meaning to the square displacement, $r^2(t)$. After each step, the randomly walking particle is temporarily trapped within a potential well. Within each well, we assume rapid "thermalization" of the particle, which therefore samples a Gaussian distribution of displacements at each site on the walk[6]. In fact, we assume this thermalization to be instantaneous, thus discarding information about high frequency intra-well dynamics. Hence, we model the time regime of α-relaxation, but not of β-relaxation.

4 Test of the GSER for small probes

We have the complex linear viscoelastic modulus for the GR model, quoted in the section above. It is now our task to compare this with the prediction of the GSER, applied to a probe particle which is representative of the fluid itself. The result of equation (1), whose validity is in doubt for a small probe of this kind, will be denoted

[4] Such phenomenology is not confirmed for conventional glass formers. However, with a high-energy cutoff in $\rho(E)$, which may be apparent in conventional glasses, Maxwellian behaviour re-appears at low ω. See Section 7.

[5] Given that the walk is Markovian, our choice of geometry of the individual steps will not influence the large-scale behaviour.

[6] We neglect modification of the Gaussian by the leaky boundary condition at the edge of the well. This is consistent with the unmodified hopping probability used to construct the GR model [11,12].

$\widetilde{G}_{\rm sp}$. Calculating $\widetilde{G}_{\rm sp}$ from equation (1) requires a knowledge of $\left\langle \widetilde{r^2}(s) \right\rangle$ in the equilibrium fluid. The brackets $\langle ... \rangle$ denote an average over all random walks of the particles, in terms of choice of path and of trap depths drawn from the prior distribution $\rho(E)$. In the absence of intra-well structure, the treatment of continuous-time random walks is discussed in references [10,24,26,27]. The mean-square displacement can be found from the correlation function C, defined by $C(\mathbf{q},t) \equiv \left\langle \mathrm{e}^{\mathrm{i}\mathbf{q}\cdot\mathbf{r}(t)} \right\rangle$. This is calculable [10] *via* $C(\mathbf{q},t) = \sum_{N=0}^{\infty} \widehat{Q}_N(\mathbf{q})\, p_t(N)$ where $p_t(N)$ is the probability of having performed exactly N hops at time t, and $\widehat{Q}_N(\mathbf{q})$ is the Fourier transform of the positional probability distribution after an N-step random walk. As described in Section 3, the positional distribution is the convolution of a standard random walk and a "Gaussian of thermalization" (whose variance is Td/k, where $k = 1$ is the local spring constant, and d the dimension of space). So its Fourier transform $\widehat{Q}_N(\mathbf{q})$ is the *product* of the usual function $\exp(-Nq^2/2)$ and another Gaussian.

The quantity $p_t(N)$ depends only on the distribution of residence times. Note that the time between hops along a random walk is drawn from the distribution $\Psi_{\rm hop}(\tau)$, which is *not* the distribution of residence times of occupied states in the system, $\Psi_{\rm occ}(\tau)$. The former distribution gives the inter-hop times *available* to a random walker upon selecting its next trap. The latter gives the residence times of all the states in the system which are *presently occupied*. Thus $\Psi_{\rm occ}(\tau)$ is related to $\Psi_{\rm hop}(\tau)$ by a weight factor τ, since the likelihood of finding a given trap occupied is proportional to the time for which it is occupied:

$$\Psi_{\rm occ}(\tau) = \frac{\tau \Psi_{\rm hop}(\tau)}{\langle \tau \rangle_{\rm hop}} \,. \tag{5}$$

Accordingly, averages of some stochastic quantity $\mathcal{Q}$ with respect to the two distributions are related by

$$\langle \mathcal{Q} \rangle_{\rm hop} = \frac{\langle \mathcal{Q}/\tau \rangle_{\rm occ}}{\langle \tau^{-1} \rangle_{\rm occ}}, \qquad \langle \mathcal{Q} \rangle_{\rm occ} = \frac{\langle \tau \mathcal{Q} \rangle_{\rm hop}}{\langle \tau \rangle_{\rm hop}} \,. \tag{6}$$

In terms of a typical random walk, $\langle \mathcal{Q} \rangle_{\rm hop}$ is the average with respect to the steps, while $\langle \mathcal{Q} \rangle_{\rm occ}$ is the average with respect to time. Note that, in calculating the probability $p_t(N)$ of having performed N hops at time t, the time spent in each trap is drawn from $\Psi_{\rm hop}(\tau)$ *except for the first trap* [26,27], which is selected from $\Psi_{\rm occ}(\tau)$. This reflects the fact that the walker is not introduced to the system at time zero, but is selected at random from the traps already occupied. This careful choice of the first trap is important to the diffusive behaviour at early times [26] and, as we shall see, its influence persists for increasingly long times as the glass transition is approached.

From the definition of $C(\mathbf{q},t)$ it follows that, in terms of its temporal Laplace transform $\widetilde{C}(\mathbf{q},s)$,

$$\left\langle \widetilde{r^2}(s) \right\rangle = -\left. \nabla_{\mathbf{q}}^2 \widetilde{C}(\mathbf{q},s) \right|_{\mathbf{q}=\mathbf{0}} \tag{7}$$

where $\nabla_{\mathbf{q}}$ denotes a derivative in $\mathbf{q}$-space. From this prescription, we find

$$\left\langle \widetilde{r^2}(s) \right\rangle = \frac{\widetilde{\Psi}_{\rm occ}(s)\, d}{s\,(1 - \widetilde{\Psi}_{\rm hop}(s))} + \frac{T\, d}{s} \,. \tag{8}$$

Here, $\widetilde{\Psi}(s)$ is the Laplace transform of $\Psi(\tau)$. The distribution of available escape times $\Psi_{\rm hop}(\tau)$ is given by averaging the exponential distribution for a single trap over the prior energy distribution $\rho(E)$ thus:

$$\Psi_{\rm hop}(\tau) = \int_0^\infty \mathrm{d}E\, \rho(E)\, \exp -[\beta E + \tau \mathrm{e}^{-\beta E}]. \tag{9}$$

So its Laplace transform is

$$\widetilde{\Psi}_{\rm hop}(s) = \left\langle \frac{1}{1 + s\overline{\tau}(E)} \right\rangle_{\rm hop} \tag{10}$$

with $\overline{\tau}(E) = \mathrm{e}^{\beta E}$ the mean residence time for trap depth E. The expression for $\widetilde{\Psi}_{\rm occ}(s)$ is the same, with the average over hops replaced by an average over occupied traps. So, from equation (6),

$$\widetilde{\Psi}_{\rm occ}(s) = \frac{1}{\langle \tau \rangle_{\rm hop}} \int_0^\infty \mathrm{d}E\, \frac{\rho(E)\overline{\tau}(E)}{1 + s\overline{\tau}(E)} = \frac{1 - \widetilde{\Psi}_{\rm hop}(s)}{s\, \langle \tau \rangle_{\rm hop}}. \tag{11}$$

Substituting this expression into equation (8) cancels the Ψ-dependence. So we see that the second moment of the distribution of displacements,

$$\left\langle \widetilde{r^2}(s) \right\rangle = \frac{Td}{s} + \frac{d}{s^2\, \langle \tau \rangle_{\rm hop}}, \tag{12}$$

is independent of any properties of the distribution of trapping times except for its mean.

If we use this expression for the self-diffusion of a small probe to calculate the modulus in equation (1) (and substitute $s = \mathrm{i}\omega$ to find the complex viscoelastic modulus in the Fourier domain), we find[7] that the GSER, applied to a small probe, predicts a complex modulus

$$G^*_{\rm sp}(\omega) = \frac{\mathrm{i}\omega\tau_0}{1 + \mathrm{i}\omega\tau_0} \qquad \text{with} \quad \tau_0 \equiv T\, \langle \tau \rangle_{\rm hop} = T / \left\langle \tau^{-1} \right\rangle_{\rm occ} . \tag{13}$$

This is *exactly* Maxwellian behaviour at all temperatures for which an equilibrium distribution exists (*i.e.* for all $T > T_{\rm g} = 1$). Clearly, this expression is completely at odds with the actual rheology of the GR model as described in Section 3.

4.1 Breakdown of the GSER

The generalized Stokes-Einstein relation, when applied to a small probe, has failed in two distinct ways which we

[7] We have set $d = 3$ and particle radius $a = k_{\rm B}/3\pi$ to simplify the constant of proportionality in the GSER (Eq. (1)).

now discuss. The first is a (fairly trivial) discrepancy in the temperature dependence, which is inherent in any hopping model. To study the spurious T-dependence of the characteristic time in equation (13), let us take the inverse Laplace transform of equation (12). Thus we find the nature of the probe's diffusive motion as a function of time:

$$\left\langle r^2(t)\right\rangle = Td + td/\left\langle \tau\right\rangle_{\rm hop}. \tag{14}$$

The time-independent term Td is the variance of the local "Gaussian of thermalization" in which the probe finds itself at each step of its walk, and respects equipartition of energy amongst the elastic degrees of freedom. The second term says that diffusion is exactly linear on all time scales[8], with a diffusion constant

$$D = \tfrac{1}{2}\left\langle \tau\right\rangle_{\rm hop}^{-1} = \tfrac{1}{2}\left\langle \tau^{-1}\right\rangle_{\rm occ}. \tag{15}$$

The GSER implies that the mean-square speed (also given by equipartition, $\left\langle \frac{1}{2}mv^2\right\rangle = \frac{1}{2}k_{\rm B}Td$) sets the rate of translation along the random walk. Indeed this is why the diffusion constant is proportional to temperature in dilute gases, where particles are not caged, so their directions rapidly become decorrelated. Like any activated hopping process [29] with a temperature-independent microscopic attempt rate (*e.g.* the Eyring model of dense fluids [30]), the GR model lacks such a factor T in the diffusion constant (Eq. (15)). This is the source of the rogue T-dependence of $G^*_{\rm sp}$. As the GR model is designed to be applied close to the glass transition, factors of T are of order unity. This source of deviation from the GSER is therefore not of great importance to most experiments, which usually only test it up to factors of order unity [13,15,19].

However, the GSER is violated by much larger factors than this arising from the second source of error in equation (13). This is the "misplacement" of the thermal averaging brackets, when compared with the correct expression in equation (3). In a Maxwellian fluid, the distribution of lifetimes is narrow, since there is a single characteristic relaxation time. Thermal averaging then commutes with the other algebraic operations, so the incorrect placement of the thermal brackets becomes irrelevant in that case[9]. However, the GSER result breaks down for broad distributions such as exist both in many real glass formers, and in the GR model. To illustrate this, let us compare the diffusion constant (Eq. (15)) with that predicted by the Stokes-Einstein relation (zero-frequency limit of the GSER), given the GR model's actual viscosity. From equation (3) with $\eta \equiv \lim_{\omega\to 0} G''(\omega)/\omega$, the SER gives the diffusion constant as $T/2\eta = T/2\left\langle \tau\right\rangle_{\rm occ}$. The first moment of the distribution of times for which traps are occupied $\left\langle \tau\right\rangle_{\rm occ}$ diverges in the GR model for temperatures below $T = 2$, whereas $\left\langle \tau^{-1}\right\rangle_{\rm occ}$, which appears in equations (15, 13), remains finite. Thus D is *enhanced* with respect to the SER value as the viscous divergence is approached, as is widely observed in experiment and simulation [16–19,23]. We note, however, that the GR model is not sufficiently elaborate to account for the power law ($1/D \propto \eta^\xi, \xi < 1$) which has been observed to replace the SER in some supercooled fluids [16].

The rheology of the GR model is equivalent to a set of over-damped harmonic oscillators (*e.g.* masses on springs in dash-pots) connected in *parallel*. Each over-damped element has the characteristics of a Maxwellian fluid, with a different time constant. Even if only a vanishingly small fraction of the population of Maxwell models becomes infinitely viscous (*i.e.* their time constants $\overline{\tau}$ diverge), it will be apparent in the response of the system, whose stress is the *sum* of stresses of the population[10]. Contrast this with the GSER for a small probe, equation (13). It claims to derive the moduli from a knowledge of only the second moment, $\left\langle r^2\right\rangle$, of the distribution of displacements. This is (qualitatively) more like summing *compliances* of the population[11].

This discussion shows that the second moment alone, $\left\langle r^2\right\rangle$, does not contain sufficient information about the distribution of displacements (or, equivalently, about the full distributions $\Psi(\tau)$) to find the rheological behaviour of the GR model. Specifically, this moment would be unaffected by a vanishingly small subset of the population being stuck for infinite time at $r = 0$; yet this subset may dominate the rheology, *e.g.* by causing $\left\langle \tau\right\rangle_{\rm occ}$ to diverge.

5 Hopping statistics in the GR model

As we have mentioned, the GR model shows some intriguing dynamical features. The viscosity diverges at a temperature ($T = 2$) well above the glass transition temperature ($T_{\rm g} = 1$ defined as the temperature below which the system has no equilibrium steady state). The diffusion constant D vanishes at $T_{\rm g}$, and yet not all particles are static below this temperature. In this section we gain a fuller picture of the model's dynamics, by investigating its hopping statistics analytically and by simulation[12].

[8] We note that the diffusive term in equation (14) is equivalent to the infinite-dimensional limit of the exact result for a random trap model on a hyper-cubic lattice obtained by Schroeder [28] and Kehr *et al.* [26,27].

[9] In fact, the GSER for small probes is tantamount to mean field theory, in which averaging indeed commutes with certain algebraic operations.

[10] The connectivity of the damped oscillators, which is parallel for the GR model (Sect. 3), will be different in many real systems, becoming a more elaborate network of series and parallel connections.

[11] Of course, the *valid* application of the GSER (to a large probe) *is* equivalent to *parallel* connection of Maxwell models, since the surface of the large probe feels the simultaneous influence of many degrees of freedom, which, within the GR model, have additive stresses.

[12] A similar analysis was carried out by Kehr *et al.* [26,27] on a real lattice (*i.e.* with spatial correlations). They modelled diffusion in crystals which exhibit no glass transition, and therefore used a distribution of residence times narrower than ours.

Let us begin by comparing the two distributions $\Psi_{\rm hop}(\tau)$ and $\Psi_{\rm occ}(\tau)$, for the residence times of particles in a trap. The first is taken over the prior distribution (of *a priori* available states); the second over those states which are actually occupied at any given time. As stated in Section 4, these two distributions are so different that selecting just the first step on a random walk from the wrong distribution can have drastic effects on $\langle r^2(t)\rangle$ which persist up to rather late times. Suppose that by mistake the *initial* residence times were drawn from the distribution $\Psi_{\rm hop}(\tau)$ (which is the correct choice for all subsequent residence times), rather than from $\Psi_{\rm occ}(\tau)$ (which is correct for the first one only [26,27]). The mean square displacement $\langle r^2(t)\rangle_{\rm prior}$ over this hypothetical ensemble has Laplace transform

$$\left\langle \widetilde{r^2}(s)\right\rangle_{\rm prior} = \frac{\widetilde{\Psi}_{\rm hop}(s)\,d}{s\,(1-\widetilde{\Psi}_{\rm hop}(s))} + \frac{T\,d}{s} \qquad (16)$$

which, in contrast to equation (12), does not depend only on the mean of the distribution $\Psi_{\rm hop}(\tau)$. The resultant $\langle r^2(t)\rangle_{\rm prior}$ is a non-linear function of time (tending to Eq. (14) as $t\to\infty$ [24]) which increases monotonically, even at $T=T_{\rm g}$ (where the true diffusion constant vanishes).

The correct value of $\langle r^2(t)\rangle$ given in equation (14) is not found as just outlined, but instead by weighting each walk in the ensemble with the residence time of the trap it is initially in [26,27]. This factor is required because the probability of a particle initially being found in a given trap is proportional to the residence time of that trap. (Since we are interested in a system which has already equilibrated, the particles have, in principle, had time to sample the distribution of traps, and are therefore more likely to be found in long-lived states than *a priori*.) It is somewhat unintuitive (though necessary as a consequence of the system's steady state) that this re-weighting of the ensemble should conspire to cancel all non-linearity from the time dependence of mean square displacements implicit in equation (16) and yield equation (14) instead.

For the exponential prior $\rho(E)=\exp(-E)$, it can be deduced straightforwardly from equations (10, 6) that, in Laplace time,

$$\widetilde{\Psi}_{\rm hop}(s) = T\int_0^\infty {\rm d}u\,\frac{{\rm e}^{-(T+1)u}}{s+{\rm e}^{-u}}$$
$$\widetilde{\Psi}_{\rm occ}(s) = (T-1)\int_0^\infty {\rm d}u\,\frac{{\rm e}^{-Tu}}{s+{\rm e}^{-u}}$$

from which it follows, showing temperature dependence explicitly, that

$$\Psi_{\rm occ}(\tau\,;\,T) = \Psi_{\rm hop}(\tau\,;\,T-1). \qquad (17)$$

Thus, at equilibrium, the residence time distribution of occupied states coincides with the prior distribution of such times at a substantially lower temperature.

5.1 Numerical results

To observe the process in action, we simulated the activated hopping of 10^5 particles, using the exponential prior distribution of trap depths $\rho(E)=\exp(-E)$. For each particle, the time interval for successive hops was drawn from $\Psi_{\rm hop}(\tau)$ (Eq. (9)) for all but the first hop (as in [26]). The algorithm used to simulate hopping in the system between times 0 and t is as follows. Each of the 10^5 particles is initially scheduled with a hopping time drawn from $\Psi_{\rm occ}(\tau)$. If this is greater than t, the particle is not visited again, and is recorded as performing zero hops during the simulation. The remaining particles are successively assigned further relaxation times[13] drawn from $\Psi_{\rm hop}(\tau)$ and their numbers of hops incremented, until the next hop is scheduled for after t. In this way the distribution $p_t(N)$ of the number N of relaxation events up to time t was measured, as a function of temperature.

The distribution of hops $p_t(N)$ gives a clearer picture of dynamics in the system than the distribution of displacements, which is just its convolution with a random walk for which $\langle r^2\rangle = Nd$. The results appear in Figure 1 for a range of temperatures and times. We see that, at high temperature, all the particles are mobile and concentrated in a peak whose position increases linearly with time. As the temperature is lowered towards the glass transition ($T=1$), a second peak containing a significant fraction of the population appears at $N=0$. Of course, as this peak decays, it feeds the rest of the distribution. Its lifetime increases as the transition is approached, yet the rest of the distribution, for which it is the source, remains concentrated in a mobile peak.

5.2 Analysis of bimodal diffusion

We consider next the time dependence of $p_t(0)$, which is the probability that the time of the first hop exceeds t:

$$p_t(0) = \int_t^\infty \Psi_{\rm occ}(\tau)\,{\rm d}\tau. \qquad (18)$$

Using equation (17) and expressing $\Psi_{\rm hop}(\tau)$ in terms of an incomplete gamma function, $\Psi_{\rm hop}(\tau) = \tau^{-(T+1)}\gamma(T+1,\tau)/T$ (from Eq. (9) with $\rho(E)={\rm e}^{-E}$), we have

$$p_t(0) = \frac{\gamma(T,t)}{t^{T-1}} + \frac{{\rm e}^{-t}}{t} \xrightarrow[t\to\infty]{} (T+1)!\,t^{-(T-1)}. \qquad (19)$$

So the population of stuck particles decays by an increasingly slow power law as the glass transition is approached. Of course, this decay is fastest at early times, so this is when the maximum in the *mobile* peak is formed. The width of the mobile peak grows with the usual square-root relation to its mean so, at late times, the population is concentrated in two distinct and narrow regions.

[13] The stochastic variable $\tau = -\xi^{-1/T}\ln\xi'$ is distributed according to $\Psi_{\rm hop}(\tau)$ if ξ and ξ' are distributed uniformly on $(0,1)$.

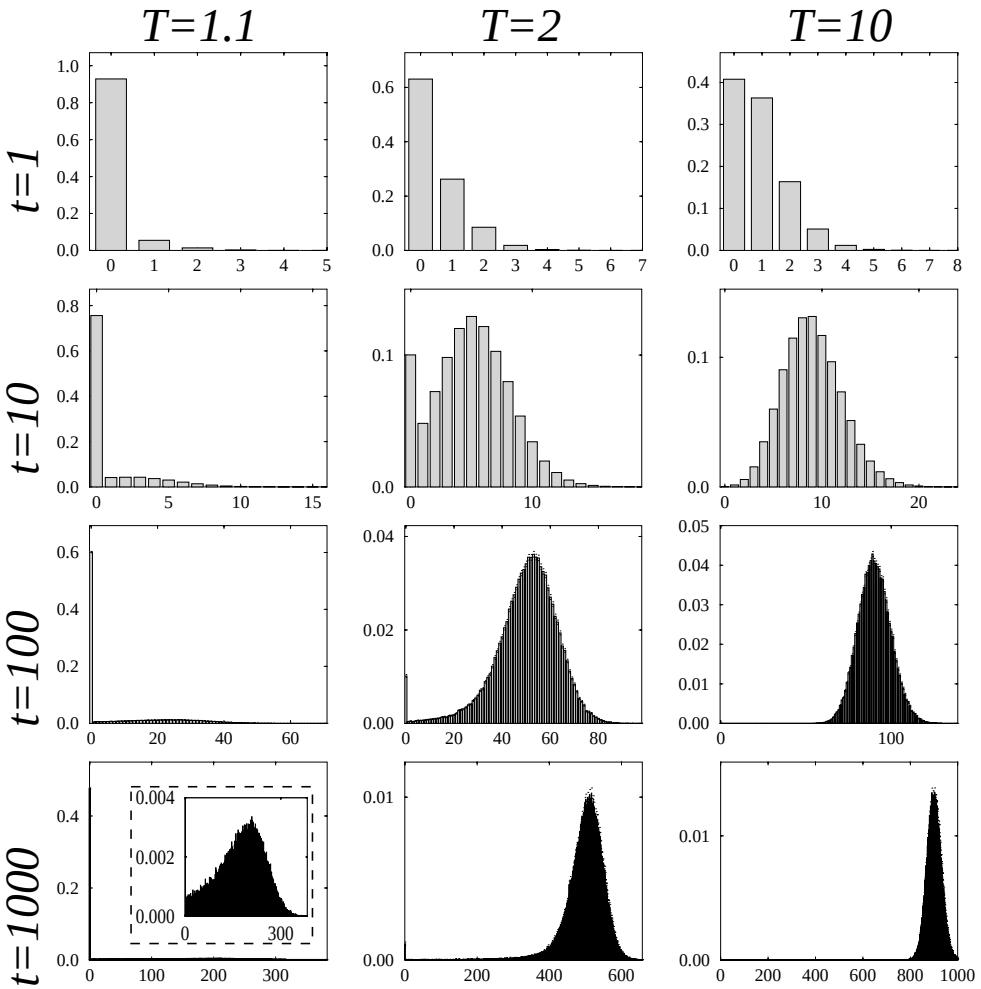

Fig. 1. Normalized distributions of number of hops performed, $p_t(N)$, in simulations at various temperatures T and times t. For $(T = 1.1, t = 1000)$, $p_t(0) = 0.476 \pm 0.002$ and the rest of the distribution is magnified in the inset.

This confirms the result of the above simulation, that the diffusion process in the GR model leads, near the glass transition, to a strongly bimodal distribution of displacements. Having hopped once, a particle is more likely to hop again in a given time, since relaxations in the mobile peak are drawn from the (effectively higher-temperature — Eq. (17)) hop distribution $\Psi_{\rm hop}(\tau)$. Nevertheless, the distribution of residence times throughout the whole system (both peaks) is $\Psi_{\rm occ}(\tau)$. Furthermore, the simulational data confirm that, although the mean of the mobile peak is a non-trivial function of time and temperature (*cf.* Eq. (16)), the two peaks together conspire to produce

$$\overline{N} = \frac{t}{\langle\tau\rangle_{\rm hop}} = \frac{T-1}{T}\,t$$

in agreement with equations (14, 15). In reference [26], such linearity in time was shown to hold in the steady state of any system of random walkers. Nevertheless, in our highly bimodal distribution, it appears somewhat remarkable.

That the "diffusion coefficient" D should actually comprise an average over two such distinct populations might call into question whether the dynamics of the model can properly be called diffusion at all: the mean square displacement may be linear in time, but is this diffusion in the ordinary sense? To address the question, we calculate the *variance* in $r^2(t)$, that is $\langle r^4\rangle - \langle r^2\rangle^2$, and find, for $1 < T < 2$,

$$\frac{\sqrt{\langle r^4\rangle - \langle r^2\rangle^2}}{\langle r^2\rangle} \xrightarrow[t\to\infty]{} \sqrt{\frac{2}{d}} + \frac{5\,\Gamma(T)}{(3-T)(2-T)\sqrt{2d}\,t^{T-1}}.$$

The leading term is the standard value for simple diffusion. The way in which this limit is approached *is* temperature dependent, but such sub-dominant terms are unlikely to impinge on experimental measurements of the diffusion constant in the ergodic ($T > 1$) system. The deviation from a Gaussian distribution of $\mathbf{r}$ at finite times is often characterized by the "non-Gaussian parameter" $A(t)$ defined [31] as

$$A(t) \equiv \frac{3}{5}\frac{\langle r^4\rangle}{\langle r^2\rangle^2} - 1$$

in 3 dimensions. Above the glass transition, this is expected [7] to vanish in the infinite-time limit. For $1 < T < 2$, we find

$$A(t) \xrightarrow[t\to\infty]{} \frac{2\Gamma(T)}{(3-T)(2-T)\,t^{T-1}}$$

whereas $A \sim 1/t$ above $T = 2$. So the non-Gaussian parameter in the GR (and Bouchaud's) model does indeed vanish, but does so increasingly slowly as the glass transition is approached. The same qualitative results were observed by (amongst others) Miyagawa *et al.* in MD simulations [32].

5.3 Timescales

We conclude this section on unforced diffusion in the GR model by summarizing the important time-scales that are present in both diffusion and rheology. The diffusion is controlled by $\langle\tau\rangle_{\rm hop}^{-1}$, equivalent to the *mean rate*, $\left\langle\tau^{-1}\right\rangle_{\rm occ}$, which vanishes linearly at $T = T_g = 1$. The *mean time* between yielding events in the system, $\langle\tau\rangle_{\rm occ}$ controls the GR model's viscosity, and diverges at $T = 2$, although the mean hopping rate is finite here. The *median* of $\Psi_{\rm occ}(\tau)$ also remains finite below $T = 2$. From equation (18), it is the time at which half the population has relaxed (when $p(0) = \frac{1}{2}$). From equation (19) this is

$$t_{\frac{1}{2}}(T) \approx [2(T+1)!]^{\frac{1}{T-1}} \tag{20}$$

which has a rather strong divergence at the glass transition ($T = 1$). Meanwhile, the *mode* of the distributions $\Psi_{\rm hop}(\tau)$ and $\Psi_{\rm occ}(\tau)$, *i.e.* the most likely time between hops, is always zero.

Given these subtle statistical properties of the self-diffusion process, which arise from the power law distribution of relaxation times in the GR model, it is no surprise that the GSER (which from Eq. (15) contains only $\langle\tau\rangle_{\rm hop}$) fails for microscopic probes.

6 Diffusion in the presence of shear

So far we have explored only the *linear* response functions of the GR model, $G^*(\omega)$ and $\langle r^2(t)\rangle$, and their interrelation. These describe any system for which the applied shear stress is either zero or so small as not to disturb thermal equilibrium. Let us now turn our attention to applied shear rates which are sufficiently large to influence self diffusion, and calculate the effect. Of course, particles in Brownian motion are also convected by the system's affine shear motion, but this effect (in which we include Taylor dispersion) can be subtracted from the overall trajectory to reveal the perturbed diffusive contribution[14]. (In simple shear, no such subtraction is needed for the component of Brownian motion transverse to the flow.) The rheology of the GR model [11,12] exhibits strong nonlinearities arising from shear-induced hops. These occur as a particle is strained within its well, and moves up the energy curve toward the yield value, making a thermal hop far more likely. Clearly such shear-induced hops could have a radical effect on the diffusive properties too. We assume that, although biased by the affine motion, each such hop still entails a random displacement whose statistics is the same as when flow is absent.

After subtraction of the affine motion, the diffusion constant is defined by $\left\langle r^2(t)\right\rangle \xrightarrow[t\to\infty]{} 2Dtd$ in d dimensions. For a random walk of N hops, $\left\langle r^2\right\rangle = Nd$ so, to calculate D, we just require the number of hops executed by an average particle in a given long time. That is,

$$2D = \lim_{t\to\infty}\left\langle\frac{N}{t}\right\rangle = \frac{1}{\langle\tau\rangle_{\rm hop}} \tag{21}$$

since the time spent in each trap along the walk[15] is drawn from $\Psi_{\rm hop}(\tau)$, and each random walk becomes typical after a sufficiently long time. We now evaluate equation (21) in the presence of shear.

Given a time-dependent macroscopic shear $\gamma(t)$, the yield rate for a trap which was entered at time t_0 was prescribed in Section 3 as

$$\Gamma_0 \exp\{-\beta(E - \tfrac{1}{2}k[\gamma(t) - \gamma(t_0)]^2)\}$$

since the trap has subsequently been sheared by an amount $l = \gamma(t) - \gamma(t_0)$. At time t, the probability of *not* having hopped from the trap of depth E entered at t_0 (which we call $f_{\rm E}(t, t_0)$) is therefore

$$f_{\rm E}(t,t_0) = \exp\left\{-\mathrm{e}^{-\beta E}\int_{t_0}^{t}\mathrm{d}t'\,\exp\left(\tfrac{1}{2}\beta[\gamma(t') - \gamma(t_0)]^2\right)\right\}$$

where $\Gamma_0 \equiv 1$ and $k \equiv 1$ as before. Integrating over the prior distribution of trap depths $\rho(E)$ gives the overall survival probability,

$$f(t,t_0) = \int_0^\infty \mathrm{d}E\,\rho(E)\,\exp\left\{-\mathrm{e}^{-\beta E}\int_{t_0}^{t}\mathrm{d}t'\,\exp\left(\tfrac{1}{2}\beta[\gamma(t')-\gamma(t_0)]^2\right)\right\}. \tag{22}$$

The conditional probability density $\psi(t\,|\,t_0)$ of hopping next at time t, given that the present trap was entered at t_0 is then

$$\psi(t\,|\,t_0) = -\frac{\mathrm{d}}{\mathrm{d}t}f(t,t_0). \tag{23}$$

[14] This applies, at least, in numerical studies, and was done in a recent MD simulation [23]. Taylor dispersion is the enhanced spreading in the flow direction arising from particles diffusing from one streamline to the next. When this and the trivial affine motion is subtracted, the remaining Brownian motion had negligible anisotropy.

[15] The hop-weighted average $\langle\tau\rangle_{\rm hop}$, which arises from the microscopic treatment, is completely equivalent to the time-weighted average $\left\langle\tau^{-1}\right\rangle_{\rm occ}^{-1}$ which arises from the Fokker-Planck equation used in references [11,12]. See equation (6).

Hence, the mean yield time, *given that the present trap was entered at time* t_0 is

$$\langle\tau\rangle_{t_0} = \int_{t_0}^{\infty} \mathrm{d}t\,(t-t_0)\,\psi(t\,|\,t_0) = \int_{t_0}^{\infty} f(t,t_0)\,\mathrm{d}t. \quad (24)$$

We next apply equations (21, 22, 24) to two particular forms of $\gamma(t)$: steady shear, $\gamma(t) = \dot\gamma\, t$, and periodic shear, $\gamma(t) = \gamma(t + 2\pi/\omega)$.

6.1 Steady shear

With a time-independent shear rate, the system reaches a steady state. (This is true for all temperatures, including those below T_g: the presence of a finite shear rate destroys weak ergodicity breaking [11,12].) Therefore, the mean relaxation time becomes independent of the time of entry into a trap. Thus equations (21, 24) are related by

$$\langle\tau\rangle_\mathrm{hop} = \langle\tau\rangle_{t_0}$$

for any t_0 we might choose. Thus we obtain

$$D^{-1} = 2\kappa^{-1}T \int_0^{\kappa^{-1}} \mathrm{d}u\,\rho(-T\ln\kappa u)\,\frac{J(u)}{u} \quad (25a)$$

$$\text{with}\quad J(u) \equiv \int_0^{\infty} \mathrm{d}\theta\,\mathrm{e}^{-u\,I(\theta)} \quad (25b)$$

$$I(\theta) \equiv \int_0^{\theta} \mathrm{d}v\,\mathrm{e}^{v^2} \quad (25c)$$

$$\text{and}\qquad \kappa^2 \equiv \dot\gamma^2/2T \quad (25d)$$

from the substitutions $u^{-1} = \kappa\,\mathrm{e}^{\beta E}$ and $\theta = \kappa\, t$. Here, κ is a re-scaled shear rate.

To proceed further we must approximate $J(u)$ (Eq. (25b)). Let us define θ_0 by $uI(\theta_0) \equiv 1$. Then for $\theta > \theta_0$, $uI(\theta)$ grows rapidly with θ, while for $0 < \theta < \theta_0$ it is small. So we can write

$$\int_0^{\infty} \mathrm{d}\theta\,\mathrm{e}^{-u\,I(\theta)} \approx \int_0^{\theta_0} \mathrm{d}\theta = \theta_0(u).$$

This approximation is equivalent to saying that shear does not greatly modify the thermal activation rate while a particle is in the bottom of a quadratic well, but yielding is immediate once the particle has been sheared to the brink of its trap. The result is

$$J(u) \approx I^{-1}(1/u) \quad (26)$$

where I^{-1} is the inverse of I in equation (25c). We now approximate this inverse function by

$$I^{-1}(y) \approx I^{-1}_\mathrm{approx}(y) \equiv \begin{cases} y & \text{for } 0 \le y < y_0 \\ 1 + \sqrt{\ln y} & \text{for } y_0 \le y \end{cases} \quad (27)$$

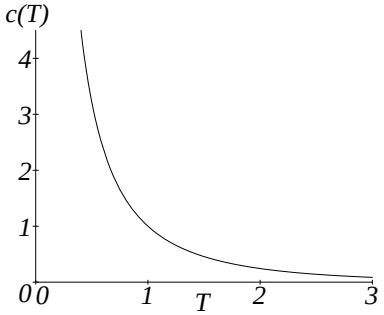

Fig. 2. The function appearing in equations (29, 30), $c(T) \equiv T^{-1}y_0^{1-T} - \frac{\sqrt{\pi}}{2}T^{-\frac{3}{2}}(T-1)\,\mathrm{erfc}\sqrt{T\ln y_0}$, where erfc is the complementary error function and $y_0 \approx 1.747$.

which is exact in the limits $y \ll 1$ and $y \gg 1$. The constant $y_0 \approx 1.747$ solves $y_0 = 1 + \sqrt{\ln y_0}$ and is the (second[16]) point of intersection of the two approximate functions. In fact, it can be shown that $I^{-1}_\mathrm{approx}(1/u)$ is always greater than $J(u)$ in equation (25a) which it approximates. So, the resulting approximation for D is a strict *lower bound*. General expressions for this are given in Appendix A. Two regimes of the scaled shear rate arise: $\kappa < y_0$ and $\kappa > y_0$.

Using the exponential prior $\rho(E)$ we find, in the limit of high shear rate,

$$D \xrightarrow[\kappa\to\infty]{} \frac{\kappa}{2\sqrt{\ln\kappa}}. \quad (28)$$

So, for fast shear, the diffusion rate is almost proportional to the shear rate. The imposed shear drags fluid elements rapidly through trap configurations, with very little time for thermal activation. More interesting behaviour occurs in the low-shear regime. With the exponential prior, the approximate (lower bound) D is (for $T < 3$ — see Appendix A)

$$D \approx \frac{(T-1)}{2T}\left[1 - \kappa^{T-1}c(T)\right]^{-1} \qquad \text{for } \kappa < y_0. \quad (29)$$

The function $c(T)$ is given in Figure 2.

Below the glass transition ($T < 1$), the diffusion constant is zero in the absence of shear, and particle motion is sub-diffusive, with $\langle r^2\rangle$ growing as some non-integer power of time [10]. However, any finite steady shear rate ensures a steady rate of yielding events and a non-zero diffusion constant. In this regime, from equation (29),

$$D \xrightarrow[\kappa\to 0]{} \frac{1-T}{2T\,c(T)}\,\kappa^{1-T}. \quad (30)$$

Thus, D is a finite, smooth function throughout all of the $(T,\dot\gamma)$ plane, except for the line segment ($\dot\gamma = 0\,,\, 0 \le T \le 1$), where it vanishes. For non-zero shear rate, there is no singularity at $T = 1$, where D becomes $-1/(2\ln\kappa)$ for low scaled shear rate κ.

[16] Choosing the other solution, $y_0 = 1$, creates an upturn in the gradient of I^{-1}, generating artefacts.

6.2 Periodic shear

A planar periodic shear strain, $\gamma(t) = \gamma(t + 2\pi/\omega)$, is experimentally more easily realizable than a constant shear rate. If we define the phase ϕ to be ωt *modulo* 2π, then we can express the mean time $\langle\tau\rangle_{t_0}$ spent in each trap on the walk (defined in Eq. (24)) as a function, $\overline{\tau}(\phi)$, only of the *phase* at which the current trap was entered. This is done in Appendix B by averaging $\langle\tau\rangle_{t_0}$ over all oscillatory cycles, for all times t_0 corresponding to phase ϕ. If $p(\phi)$ is the probability that a trap was entered at phase ϕ of the cycle, then the mean residence time in equation (21) is

$$\langle\tau\rangle_{\rm hop} = \int_0^{2\pi} \mathrm{d}\phi\, p(\phi)\, \overline{\tau}(\phi). \tag{31}$$

Let $p(\phi\,|\,\phi_0)$ be the *conditional* probability density of a hop occurring at phase ϕ, *given* that the previous hop was at ϕ_0. Then $p(\phi)$ is the (normalized) solution to the integral equation

$$p(\phi) = \int_0^{2\pi} p(\phi\,|\,\phi_0)\, p(\phi_0)\, \mathrm{d}\phi_0. \tag{32}$$

The quantities $p(\phi\,|\,\phi_0)$ and $\overline{\tau}(\phi)$ have simple relations to the distribution $\psi(t\,|\,t_0)$ given in equation (23). In Appendix B they are given in terms of a single cycle of the imposed waveform.

Equation (32) is a homogeneous Fredholm equation of the second kind, for which the general solution is not known. However, the problem greatly simplifies in the limit of small amplitude oscillations, which we now treat. (Note that this perturbative treatment is only possible for $T > 1$, where an unperturbed steady state exists.) In the absence of shear $p(\phi)$ and $\overline{\tau}(\phi)$ must be independent of ϕ. In that case, we write $p(\phi) = 1/2\pi$ and $\overline{\tau}(\phi) = \overline{\tau}_0$. If the oscillatory shear creates only small perturbations $\Delta p(\phi) = p(\phi) - 1/2\pi$ and $\Delta\overline{\tau}(\phi) = \overline{\tau}(\phi) - \overline{\tau}_0$, then equation (31), to first order in small quantities, becomes

$$\langle\tau\rangle_{\rm hop} = \frac{1}{2\pi}\int_0^{2\pi} \overline{\tau}(\phi)\, \mathrm{d}\phi. \tag{33}$$

We have used the fact that p is normalized, so that $\int_0^{2\pi} \Delta p(\phi)\, \mathrm{d}\phi = 0$. Hence we need only expand equation (B.2) to lowest order in strain amplitude and average it over a cycle to find $\langle\tau\rangle_{\rm hop}$ and hence the diffusion constant. The result for an exponential prior $\rho(E) = \exp(-E)$ and sinusoidal shear of amplitude γ_0 is

$$D^{-1} = \frac{2T}{T-1} - \gamma_0^2\, \omega^{T-1} \int_0^{\omega^{-1}} \frac{u^{T-2}}{1+u^2}\mathrm{d}u + \mathcal{O}(\gamma_0^4). \tag{34}$$

For $T < 3$, the integral is convergent as $\omega \to 0$. In fact, for *any* waveform, the low-frequency limit for an exponential prior is

$$D^{-1} \xrightarrow[\omega\to 0]{} \frac{2T}{T-1} - \gamma_0^2\, \omega^{T-1}\, g(T) + \mathcal{O}(\gamma_0^4) \tag{35}$$

where, in the sinusoidal case, $g(T) = (\pi/2)\,\mathrm{cosec}\,[(T-1)\pi/2]$. In the high-frequency limit, equation (34) yields instead

$$D^{-1} \xrightarrow[\omega\to\infty]{} \frac{2T - \gamma_0^2}{T-1} + \mathcal{O}(\gamma_0^4).$$

For larger amplitudes, we can use the results of Section 6.1. Given a sufficiently low frequency ($\omega \ll D$), the shear rate at any given point on the cycle is almost constant. In that case, the steady-shear expressions for D^{-1} can be averaged over a sinusoidal cycle, yielding (for $\omega \ll D$)

$$D \approx \frac{T-1}{2T}\left[1 - (\omega\,\gamma_0)^{T-1} h(T)\right]^{-1};\ \ \gamma_0^2\omega^2 < 2T \tag{36}$$

and, to within logarithmic factors,

$$D \propto \omega\,\gamma_0\ ; \qquad \gamma_0^2\omega^2 \gg 2T \tag{37}$$

where $h(T) \equiv 2^{(T-1)/2} c(T)\, B(T/2, T/2)/\pi$, c is given in Figure 2 and B is Euler's integral of the second kind.

We now summarize the effects, calculated above, of low-frequency periodic shear on diffusion just above the glass transition. For the smallest amplitudes γ_0, we expect the change in the diffusion constant to be proportional to $\gamma_0^2\,\omega^{T-1}$. At larger amplitude, this should cross over to $(\gamma_0\,\omega)^{T-1}$, and at the largest amplitudes, D is almost proportional to $\omega\,\gamma_0$. We interpret these three regimes as follows. The smallest oscillations serve only to vibrate particles within the bottoms of their quadratic potential wells, thus effectively making all wells just a little shallower. Larger amplitude strains cause yielding of even the deepest wells in the time taken for the affine shear to reach the yield point. However, the part of the population in the shallowest wells are thermally activated more quickly than this affine shear time-scale. The dividing line between those two parts of the population depends on the shear rate. At the highest shear rates, the global affine shear accounts for almost all yielding.

7 Discussion and conclusion

We have studied quantitatively, within a simple hopping model of glassy dynamics, the relation between diffusion and rheological responses (in the linear response regime) and (for the nonlinear regime) the coupling between these two aspects of the dynamics.

In the presence of a broad distribution of relaxation times, as the model possesses (and as is generic in hopping models of the glass transition) one can expect strong violations of the generalized Stokes-Einstein relation (Eq. (1)) when applied [15] to the self-diffusion of representative particles in the medium (small probes). The relation holds only for probe particles large enough that their surroundings are properly viewed as a continuum [14]. Effective-medium theories, and also simple forms of mode-coupling

theory [2] (in which a single mode of slow relaxation dominates) can give misleading predictions under these conditions. For glassy systems, use of the GSER will underpredict the diffusivity of particles and/or the rheological viscoelastic moduli. This is because the latter are dominated by the most immobile and the former is dominated by the most mobile particles.

In fact, the nature of diffusion in the model is quite subtle (see Sect. 5): close to (but above) the glass transition one has an apparently bimodal behaviour. Starting from any initial equilibrium state, a fraction of particles remain stuck for a long time, but any particle that has hopped once remains mobile thereafter. It is peculiar that, despite this, the diffusive behaviour conspires to be relatively normal (at least for low order moments of the displacement distribution; moments of fractional negative order would presumably reveal a different story).

An additional peculiarity of diffusion, which our model does not include, but which could also lead to enhanced diffusivity near the glass temperature, has been observed in a recent molecular dynamics simulation [33]. In reference [33] the effective dimensionality of the most mobile random walks was observed to decrease with temperature. At low temperature, particles moved along string-like clusters (also seen in Ref. [23]), and therefore covered greater distances than in an uncorrelated random walk in three dimensions.

We have also applied our GR model to calculate the change in the self-diffusion constant when a material is sheared. After subtraction of affine motion (including Taylor dispersion) [23], or equivalently restricting attention to diffusion perpendicular to the shear direction, one finds a strong effect of imposed flow on the mean jump rate [12] and hence on the diffusion constant. The effect is particularly extreme below the glass transition, where an anomalous (sub-diffusive) behaviour is converted to a finite diffusivity which has, instead, a power law dependence on the steady shear rate. Such effects should be accessible in scattering experiments (with wavevector almost perpendicular to the flow direction) on labelled small probes. In oscillatory shear, an enhancement in D was predicted in Section 6 for systems above (but near) the glass temperature; this could also be probed *via* scattering.

The GR model as described in Section 3 was originally developed in reference [11] to reproduce the generic rheology of a class of "soft glassy materials". (We comment further below on its relevance to conventional glasses.) This class was argued to include, for example, foams, emulsions, pastes and slurries. Experimentally, their linear viscoelastic behaviour is often characterized by a nearly constant ratio of the elastic and loss moduli $G'(\omega)$, $G''(\omega)$ (G''/G' is usually about 0.1) with a frequency dependence that is either a weak power law (clay slurries, paints, microgels) or negligible (tomato paste, dense emulsions, dense multilayer vesicles) [34]. This behaviour persists down to the lowest experimentally accessible frequencies. Sometimes a regime is seen at small ω where G' is constant and G'' is decreasing (which can be interpreted in terms of the model's behaviour below T_g [11,12,25]).

As mentioned in Sections 1 and 3, there are two differences between the GR model used in this paper and its soft counterpart in [11]. The first is that the *soft* GR model refers not to particles, as we have done, but to mesoscopic material "elements", large enough for a local elastic strain variable to be defined but small enough to have strong heterogeneity in local yield energies. (For the case of a foam, say, an "element" could correspond to a domain of several bubbles, and "yield" to a local topological change.) It is not necessarily clear what is meant by self-diffusion of such elements, so in the present paper we have retained a particle picture, although this is more natural for conventional glass-forming liquids than for soft glassy materials.

The second difference is that in the *soft* GR model, T is replaced by an effective "noise temperature" x. It was argued in [11] that the resemblance to thermal activation is formal: the "activated" yield processes are viewed as arising primarily by coupling to structural rearrangements elsewhere in the system. Indeed, the elastic energies associated with local rearrangements in foams and the like are many orders of magnitude in excess of k_BT, so any interpretation of x as a true temperature is somewhat unconvincing for these materials (in contrast to conventional glasses). Although this interpretation remains problematical, as discussed in [11,12], with it the soft GR model is able to reproduce many of the rheological properties of soft glassy materials.

The results we have obtained for the GR model, concerning breakdown of the GSER and the nature of shear-induced diffusion, equally apply (with $T \to x$) to the *soft* GR model. The breakdown of GSER, arising from the fact that diffusion and rheology probe different aspects of the relaxation spectrum, is equally natural in this case; the other contribution to its breakdown discussed in 4.1, arising from the temperature dependence of the local attempt frequency, even more so (since x is anyway not a true temperature). The results of Section 6 for shear-induced diffusion could also be quite interesting for soft glassy materials, in which it is easy to apply shear strains large enough to strongly perturb the intrinsic relaxation times. The length scales in these materials can be probed *via* light scattering; index matching is often possible so that true tracer diffusion (of a small subset of unmatched droplets or particles) can be measured [35]. For oscillatory flows, an important innovation is the echo technique [36] in which the positions of a given scatterer at identical points in the shear cycle are compared.

Results on dense emulsions [36] suggest, in fact, that not only are shear-induced reorganizations easily detectable, but that these have strong temporal and spatial correlations — regions that reorganize at a given point in the shear cycle will do so again in the next one. Such correlations are not included in the (soft) GR model(s) although they might be added in principle [38]. (It would require escape from a shallow trap to be preferentially into another shallow trap, though we do not advocate appending such *ad hoc* correlations to this simplified model.) It would be very interesting to know whether the same applies in conventional glasses; preliminary work on colloidal

suspensions (which are traditionally thought of in these terms) suggests not [37].

Finally, we return to the phenomenology of the GR model in relation to conventional glass-forming liquids. As explained in Section 3.2, the GR model in its basic form predicts a viscosity divergence at $T = 2$, while the diffusion constant vanishes only at $T = 1$, where the system has a glass transition to a non-ergodic state. This existence of a temperature range with finite diffusivity but infinite viscosity appears to be at odds with the experimentally observed behaviour of conventional glasses. A common divergence of viscosity and inverse diffusion constant can however be incorporated into the GR model through a cutoff $E_{\max}$ on the distribution of yield energies $\rho(E)$; this modification of the model has in fact already been discussed in reference [12]. It yields a viscosity which initially follows the original power-law divergence as $T = 2$ is approached, but then crosses over to $\eta \sim \exp(E_{\max}/T)$ as T is lowered further. Similarly, the predicted $1/D$ would first seem to diverge as $T = 1$ is approached from above, but actually remain finite there and eventually approach infinity at the same temperature as the viscosity ($T = 0$). The shear moduli obey the power laws (Eq. (4)) down to a cutoff frequency $\omega_{\min} = \exp(-E_{\max}/T)$, but then cross over to low-frequency Maxwell behaviour ($G' \sim \omega^2$, $G'' \sim \omega$).

The above simple temperature dependences apply if, as we did throughout, we assume that the (prior) density of yield energies is temperature independent. This is of course an approximation; Odagaki, for example, suggested that the width of $\rho(E)$ may in fact scale as the inverse of the amount of free volume $v(T)$ in the system [8]. In all temperature dependences, $T\,v(T)$ then replaces T. As a consequence, if the free volume decreases smoothly to zero at a finite temperature $T_{\rm VF}$, a Vogel-Fulcher-like divergence of η and $1/D$ at $T_{\rm VF}$ (rather than the above Arrhenius behaviour) would be predicted by the GR model with energy cutoff. One would then be inclined to locate the glass transition at that point; if we revert to temperature independent $\rho(E)$, this corresponds to $T = 0$ (rather than $T = 1$, which is the appropriate choice in the absence of an energy cutoff). Results in the range $0 < T < 1$ for the GR model with cutoff may therefore actually apply to supercooled liquids *above* the glass transition. These include a dynamic modulus $G^*(\omega)$ which becomes *more* Maxwellian in the low-frequency range as T is lowered (for $T < 1$, one has $G' \sim$ const. and $G'' \sim \omega^{T-1}$ above the cutoff frequency $\omega_{\min}$ [12], and hence Maxwell behaviour with relaxation time $1/\omega_{\min}$ for $T \to 0$), in an intriguing correspondence with data taken by Menon *et al.* [39].

This work was funded by EPSRC Grant No. GR/K56025 (RMLE) and a Royal Society Dorothy Hodgkin fellowship (PS). We wish to thank P. N. Pusey, F. Lequeux, P. Hébraud and J.-P. Bouchaud for helpful discussions.

Appendix A: General expressions for the diffusion constant under steady shear

Substituting equations (26, 27) into (25a) yields lower bounds on D (upper bounds on D^{-1}) in two regimes:

$$D^{-1} < 2\kappa^{-1}T \int_0^{\kappa^{-1}} \mathrm{d}u\, \frac{\rho(-T\ln\kappa u)}{u} \left(1+\sqrt{\ln u^{-1}}\right) \quad \text{for } \kappa > y_0 \qquad \text{(A.1)}$$

$$D^{-1} < 2\kappa^{-1}T \int_0^{y_0^{-1}} \mathrm{d}u\, \frac{\rho(-T\ln\kappa u)}{u} \left(1+\sqrt{\ln u^{-1}}\right) + 2\kappa^{-1}T \int_{y_0^{-1}}^{\kappa^{-1}} \mathrm{d}u\, \frac{\rho(-T\ln\kappa u)}{u^2} \quad \text{for } \kappa < y_0. \qquad \text{(A.2)}$$

In each case, D is approximately equal to the lower bound for $T < 3$.

Appendix B: Evaluation of the phase-dependent relaxation time and conditional probability under periodic strain

The probability of leaving a trap at time t given that it was entered at t_0 (at phase $\phi_0 = \omega t_0 \bmod 2\pi$ of the oscillatory cycle) is $\psi(t\,|\,t_0)$. Hence the mean time spent in the trap, given that it was entered at phase ϕ_0, is

$$\overline{\tau}(\phi_0) = \int_{\phi_0/\omega}^{\infty} (t - \phi_0/\omega)\ \psi(t\,|\,\phi_0/\omega)\,\mathrm{d}t$$

which, from equation (23), gives

$$\overline{\tau}(\phi_0) = \int_{\phi_0/\omega}^{\infty} f(t, \phi_0/\omega)\,\mathrm{d}t$$

with f defined in equation (22). For compact notation, we define $a(\omega t) \equiv \gamma(t)/\sqrt{2T}$ and $\tau_E(\phi_0)$ according to

$$\overline{\tau}(\phi_0) \equiv \int_0^{\infty} \rho(E)\,\tau_E(\phi_0)\,\mathrm{d}E.$$

Thus we find

$$\omega\ \tau_E(\phi_0)|_{E=-T\ln\omega u} = \int_{\phi_0}^{\infty} \mathrm{d}\phi\, \exp\left\{-u\int_{\phi_0}^{\phi} \mathrm{d}\phi'\ \exp[a(\phi') - a(\phi_0)]^2\right\}. \qquad \text{(B.1)}$$

Since $\exp[a(\phi') - a(\phi_0)]^2$ is a periodic function of ϕ, the integrand in equation (B.1) increases by a constant factor with each cycle $\phi \to \phi + 2\pi$. Thus the R.H.S. is a geometric series of integrals over a single cycle,

$$\left\{\sum_{n=0}^{\infty}\left[\exp\left(-u\int_0^{2\pi}\mathrm{d}\phi'\ \exp[a(\phi') - a(\phi_0)]^2\right)\right]^n\right\} \times \int_{\phi_0}^{\phi_0+2\pi} \mathrm{d}\phi\, \exp\left\{-u\int_{\phi_0}^{\phi}\mathrm{d}\phi'\ \exp[a(\phi') - a(\phi_0)]^2\right\}.$$

Finally, $\overline{\tau}(\phi_0)$ is expressed in terms of a single cycle as

$$\overline{\tau}\,(\phi_0) = \frac{T}{\omega}\int_0^{\omega^{-1}} \mathrm{d}u\,\frac{\rho(-T\ln\omega u)}{u}\int_0^{2\pi}\mathrm{d}\phi \qquad \text{(B.2)}$$
$$\times\frac{\exp\left\{-u\int_{\phi_0}^{\phi+2\pi\Theta(\phi_0-\phi)}\mathrm{d}\phi'\,\exp[a(\phi')-a(\phi_0)]^2\right\}}{1-\exp\left\{-u\int_0^{2\pi}\mathrm{d}\phi'\,\exp[a(\phi')-a(\phi_0)]^2\right\}}$$

where $\Theta(\phi_0-\phi)$ is the Heaviside step function.

Similarly,

$$p(\phi\,|\,\phi_0) = \int_{\phi_0/\omega}^{\infty}\delta([\omega t \bmod 2\pi]-\phi)\;\psi(t\,|\,\phi_0/\omega)\;\mathrm{d}t$$

(with $\delta(x)$ the Dirac delta function) is also a geometric series, from which it follows

$$p\,(\phi\,|\,\phi_0) = T\int_0^{\omega^{-1}}\mathrm{d}u\,\rho(-T\ln\omega u)\,\frac{\mathrm{d}}{\mathrm{d}\phi} \qquad \text{(B.3)}$$
$$\times\frac{\exp\left\{-u\int_{\phi_0}^{\phi+2\pi\Theta(\phi_0-\phi)}\mathrm{d}\phi'\,\exp[a(\phi')-a(\phi_0)]^2\right\}}{1-\exp\left\{-u\int_0^{2\pi}\mathrm{d}\phi'\,\exp[a(\phi')-a(\phi_0)]^2\right\}}.$$

References

1. C.A. Angell, Science **267**, 1924 (1995).
2. W. Kob, in *Experimental and Theoretical Approaches to Supercooled Liquids: Advances and Novel Applications*, edited by J. Fourkas, D. Kivelson, U. Mohanty, K. Nelson (ACS Books, Washington, 1997); W. Götze, in *Liquids, Freezing and Glass Transition, Les Houches Session LI*, edited by J.-P. Hansen, D. Levesque, J. Zinn-Justin (Elsevier Science Pub., 1989), Chap. 5; W. Götze, L. Sjögren, Z. Phys. B **65**, 415 (1987).
3. J.-P. Bouchaud, M. Mézard, Prog. Theor. Phys. Sup. **126**, 181 (1997).
4. J.-P. Bouchaud, J. Phys. I France **2**, 1705 (1992).
5. P. Sibani, `cond-mat/9706232` (unpublished).
6. E. Rossler, M. Taupitz, H.M. Vieth, J. Phys. Chem. **94**, 6879 (1990).
7. T. Odagaki, J. Matsui, Y. Hiwatari, Physica A **204**, 464 (1994).
8. T. Odagaki, Phys. Rev. Lett. **75**, 3701 (1995).
9. H. Scher, M.F. Shlesinger, J.T. Bendler, Phys. Today **44**, 26 (1991) and references therein.
10. C. Monthus, J.-P. Bouchaud, J. Phys. A **29**, 3847 (1996).
11. P. Sollich, F. Lequeux, P. Hébraud, M.E. Cates, Phys. Rev. Lett. **78**, 2020 (1997).
12. P. Sollich, Phys. Rev. E **58**, 738 (1998).
13. F. Gittes, B. Schnurr, P.D. Olmsted, F.C. MacKintosh, C.F. Schmidt, Phys. Rev. Lett. **79**, 3286 (1997); T.G. Mason, K. Ganesan, D. Wirtz, S.C. Kuo, Phys. Rev. Lett. **79**, 3282 (1997).
14. B. Schnurr, F. Gittes, F.C. MacKintosh, C.F. Schmidt, Macromolecules **30**, 7781 (1997).
15. T.G. Mason, D.A. Weitz, Phys. Rev. Lett. **74**, 1250 (1995); T.G. Mason, Gang Hu, D.A. Weitz, J. Opt. Soc. Am. A **14**, 139 (1997).
16. F. Fujara, B. Geil, H. Sillescu, G. Fleischer, Z. Phys. B **88**, 195 (1992).
17. D. Ehlich, H. Sillescu, Macromolecules **23**, 1600 (1990).
18. F.H. Stillinger, J.A. Hodgdon, Phys. Rev. E **50**, 2064 (1994).
19. M.T. Cicerone, M.D. Ediger, J. Chem. Phys. **104**, 7210 (1996).
20. M.T. Cicerone, P.A. Wagner, M.D. Ediger, J. Phys. Chem. B **101**, 8727 (1997).
21. E. Rossler, Phys. Rev. Lett. **65**, 1595 (1990).
22. G. Maret, P.E. Wolf, Z. Phys. B **65**, 409 (1987); D.J. Pine, D.A. Weitz, P.M. Chaikin, E. Herbolzheimer, Phys. Rev. Lett. **60**, 1134 (1988); D.J. Durian, Phys. Rev. E **51**, 3350 (1995).
23. R. Yamamoto, A. Onuki, Europhys. Lett. **40**, 61 (1997); R. Yamamoto, A. Onuki, `cond-mat/9806207` (unpublished).
24. J.-P. Bouchaud, A. Georges, Phys. Rep. **195**, 127 (1990).
25. S. Fielding, P. Sollich, M.E. Cates (to be published).
26. K.W. Kehr, D. Richter, R.H. Swendsen, J. Phys. F **8**, 433 (1978).
27. J.W. Haus, K.W. Kehr, Phys. Rep. **150**, 263 (1987).
28. K. Schroeder, in *Proceedings of the International Conference on Fundamental Aspects of Radiation Damage in Metals, ERDA CONF751006, Volume 1*, edited by M.T. Robinson, F.W. Young Jr. (1975), p. 525. See also K.W. Kehr, T. Wichmann, Mater. Sci. Forum **223**, 151 (1996).
29. See *e.g.* M. Goldstein, J. Chem. Phys. **51**, 3728 (1969) and reference [21] for a discussion of activated transport at low temperature.
30. See *e.g.* D. Tabor, *Gases, Liquids and Solids*, 3rd edn. (Cambridge Uni. Press, 1991).
31. A. Rahman, K.S. Singwi, A. Sjölander, Phys. Rev. **126**, 986 (1962).
32. H. Miyagawa, Y. Hiwatari, Phys. Rev. A **44**, 8278 (1991).
33. C. Donati, J.F. Douglas, W. Kob, S.J. Plimpton, P.H. Poole, S.C. Glotzer, Phys. Rev. Lett. **80**, 2338 (1998).
34. M.R. Mackley, R.T.J. Marshal, J.B.A.F. Smeulders, F.D. Zhao, Chem. Engin. Sci. **49**, 2551 (1994); R.J. Ketz, R.K. Prudhomme, W.W. Graessley, Rheol. Acta **27**, 531 (1988); S.A. Khan, C.A. Schnepper, R.C. Armstrong, J. Rheol. **32**, 69 (1988); T.G. Mason, J. Bibette, D.A. Weitz, Phys. Rev. Lett. **75**, 2051 (1995); P. Panizza *et al.*, Langmuir **12**, 248 (1996); H. Hoffmann, A. Rauscher, Coll. Polym. Sci. **271**, 390 (1993).
35. W. van Megen, S.M. Underwood, I. Snook, J. Chem. Phys. **85**, 4065 (1986); W. van Megen, S.M. Underwood, J. Chem. Phys. **88**, 7841 (1988); W . van Megen, S.M. Underwood, J. Chem. Phys. **91**, 552 (1989). For recent work on the glassy dynamics of hard sphere systems, see also van Megen, Transport Theory and Stat. Phys. **24**, 1017 (1995) and references therein.
36. P. Hebraud, F. Lequeux, J.P. Munch, D.J. Pine, Phys. Rev. Lett. **78**, 4657 (1997).
37. M.D. Haw, W.C.K. Poon, P.N. Pusey, P. Hebraud, F. Lequeux, Phys. Rev. E **58**, 4673 (1998).
38. For related ideas see M.L. Falk, J.S. Langer, Phys. Rev. E **57**, 7192 (1998).
39. N. Menon, S.R. Nagel, D.C. Venerus, Phys. Rev. Lett. **73**, 963 (1994).